

Plume-lithosphere interaction beneath a fast moving plate

Catherine Thoraval,¹ Andréa Tommasi,¹ and Marie-Pierre Doin²

Received 11 July 2005; revised 12 October 2005; accepted 25 October 2005; published 5 January 2006.

[1] Two-dimensional numerical simulations of mantle convection with temperature and pressure dependent viscosity are used to study plume–lithosphere interaction beneath a fast moving plate. Plumes behavior and, hence, their erosional and melting potential, depend on the Rayleigh number and plume buoyancy flux. Analysis of the balance between large-scale and plume-induced flow and of the ability of the plume to melt allows to put bounds on the upper mantle viscosity (10^{20} , 10^{21} Pas), on the plumes diameter (<200 km) and temperature anomaly (200 – 400°C). Within this range of parameters, strongly time-dependent small-scale instabilities form in the plume-lithosphere boundary layer. They lead to thermal rejuvenation of the lithosphere downstream from the plume. The 1200°C isotherm is raised by up to 30km , but the 800°C isotherm is hardly moved, leading to a steep transient geotherm at the base of the plate. **Citation:** Thoraval, C., A. Tommasi, and M.-P. Doin (2006), Plume-lithosphere interaction beneath a fast moving plate, *Geophys. Res. Lett.*, *33*, L01301, doi:10.1029/2005GL024047.

1. Introduction

[2] Mantle plumes are assumed to be thermal and/or chemical instabilities ascending through the convecting mantle. The impact of a plume head beneath the lithosphere is generally thought to result in intense melting of plume material, producing large igneous provinces. In a later stage, decompression melting in the plume tail results in hotspot volcanic chains as the lithosphere moves above it. Despite their numerous signatures at the surface, the processes taking place at the plume-lithosphere boundary layer are still poorly understood. A major open question regards the ability of a plume to significantly erode the lithosphere.

[3] Observations of the lithosphere thickness and erosion atop mantle plumes are highly controversial. Seismic studies beneath Hawaii lead to opposite conclusions. Surface-wave dispersion as well as sP converted waves data require no significant thinning, but very low velocities in the asthenosphere [Bock, 1991; Woods *et al.*, 1991; Woods and Okal, 1996; Priestley and Tilmann, 1999]. On the other hand, recent S-wave receiver function data image a gradual thinning of the lithosphere from the present hotspot location, beneath Hawaii, towards Kauai, where the lithosphere is reduced by half [Li *et al.*, 2004]. Heat flow data also lead to contradictory conclusions. Comparison of on-swell and off-swell data for the Hawaii hotspot points to no significant thermal rejuvenation of the lithosphere above

the plume [Von Herzen *et al.*, 1989]. A small increase of surface heat flow (5 – 10 m W m^{-2}) is nevertheless observed below the Cabo Verde, Bermuda, and La Reunion hotspot tracks, suggesting some lithospheric thinning downstream of the actual hotspot location [Bonneville *et al.*, 1997].

[4] 2D and 3D numerical models performed under steady-state or quasi steady-state conditions show that thermo-mechanical erosion of the lithosphere above a mantle plume is a slow process and hence turn out significant reheating of the lithosphere beneath a moving plate [Monnereau *et al.*, 1993; Davies, 1994; Ribe and Christensen, 1994, 1999; Sleep, 1994]. In contrast, recent 3D numerical models suggest that the strongly time dependent small-scale convective instabilities in the low-viscosity layer formed by the spreading of hot plume material at the base of the lithosphere may be an effective mechanism to erode the base of the lithosphere, even for a fast-moving plate like the Pacific [Moore *et al.*, 1998]. However, viscosity in these models shows a much lower temperature-dependence than the one expected in upper mantle based on laboratory deformation experiments [Karato and Wu, 1993], leading to underestimated lithosphere viscosities.

[5] In this paper, 2D Cartesian numerical convection models are used to further study the plume-lithosphere interaction beneath a fast-moving plate. Convective destabilisation of the lithosphere by the plume and, hence, the erosion of the lithosphere, are described as a function of the plume buoyancy flux and of the global Rayleigh number. The ability of modelled plumes to produce partial melting is used to discriminate Earth-like plumes.

2. Model

[6] Small-scale convection is a highly time-dependent feature, associated with strong viscosity gradients, which description requires time-costly models with very fine grids. Thus to investigate a large range of Rayleigh numbers and plume buoyancy fluxes, we performed 25 numerical experiments using a 2D convection code [Christensen, 1983, 1984].

[7] The modeled domain has open bottom and downstream side boundaries. A velocity field is imposed on top to mimic plate motion (the ridge is located at the upper-left corner). Constant temperature is imposed on top and bottom sides. Internal heating is not taken into account. The numerical grid consists of rectangular elements of variable size. The grid is refined horizontally where the plume is to be introduced and vertically at the top of the box to avoid numerical artifacts and to achieve a better description of the plume-lithosphere interaction. The calculations are performed in a non-dimensional space. The re-dimensionalisation scheme is based on the box thickness and on the temperature drop from the bottom to the top of the box (fixed to

¹Laboratoire de Tectonophysique, Université Montpellier 2, Montpellier, France.

²Laboratoire de Géologie, Ecole Normale Supérieure, Paris, France.

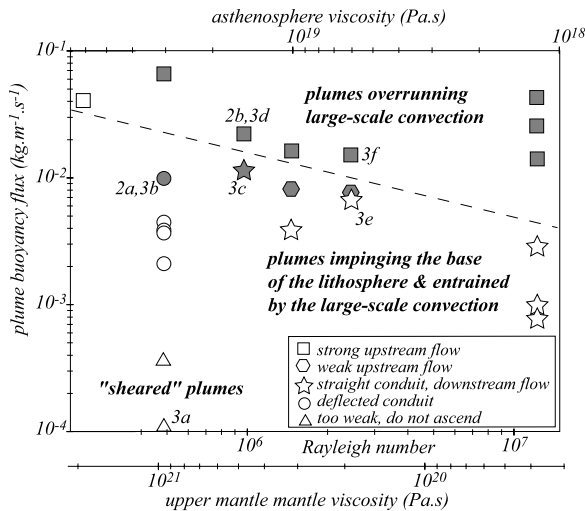


Figure 1. Regime diagram describing the plume behavior as a function of the Rayleigh number and of the 2D plume buoyancy flux. Gray symbols mark plumes that produce anhydrous melting. Labels identify the models presented in Figures 2 and 3.

$H = 700$ km and $\Delta T_B = 1350^\circ\text{C}$ respectively). The aspect ratio of the box is 1/10. The age of the lithosphere at the upper right corner is ca. 95 m.y. for a plate velocity of 13.5 cm/y. The minimum grid step for most models is < 7 km, but resolution tests have also been performed with a minimum grid step of 4 km.

[8] The viscosity is Newtonian and depends exponentially on temperature and pressure according to the following equation $\nu = \nu_0 e^{\left(\frac{E_a + V_a P}{RT}\right)}$. The activation energy E_a and the activation volume V_a have been set to 250 kJ/mol and $2.25 \text{ cm}^3/\text{mol}$, ν_0 is a reference viscosity and R is the gas constant. Rayleigh number (Ra) varies from 2.10^5 to 1.10^7 , corresponding to viscosities at the bottom of the box (ν_B) of 4.10^{19} and 2.10^{21} Pa s according to $Ra = \frac{\alpha \rho g \Delta T_B H^3}{\kappa \nu_B}$ where α is the thermal expansivity, ρ the density and κ the thermal diffusivity respectively set to 3.10^{-5} K^{-1} , 3300 kg/m^3 and $1.10^{-6} \text{ m}^2/\text{s}$. The specific heat is set to 1250 J/kg K .

[9] Initial conditions are obtained by running the model without plume until equilibrium is reached. The plate motion is responsible for a large-scale flow. The lithosphere first cools following the half-space model. After an onset time, function of Ra , small-scale convection develops, leading to a constant lithosphere thickness at old ages [Davaille and Jaupart, 1994; Dumoulin et al., 2001]. Small-scale convection develops within the modeled domain for Ra higher than 2.10^6 .

[10] Since we want to study the interaction of an ongoing plume with the lithosphere and not the plume initiation process, the plume is introduced as a bottom temperature patch with a Gaussian temperature profile, located at the middle of box. This may represent a plume originating at the base of the transition zone or a steady plume conduit ascending from deeper in the mantle. Some Pacific plumes, such as Hawaii, are believed to originate deep in the lower mantle, while others may have a shallower source [Steinberger, 2000; Courtillot et al., 2003]. For instance, the

hotspots in the South Pacific Superswell might come from the transition zone, in relation with the large region of slow seismic velocities extending throughout the lower mantle [Davaille, 1999].

[11] Each plume is characterized by its maximum temperature anomaly ΔT and by its diameter \emptyset , defined by the position at which the temperature anomaly is reduced by a factor e . Diameters range from 35 km to 200 km. Recent magnetotelluric data require that the radius of the Hawaii plume is less than 100 km [Constable and Heinson, 2004]. A maximum plume radius of 70 km is also deduced from the sharpness of the bend in the Hawaiian-Emperor hotspot track [Duncan and Richards, 1991]. In contrast, recent seismic tomography images of mantle plumes show conduits with radius between 100–400 km extending throughout the mantle [Montelli et al., 2004]. Temperature anomalies vary between 100°C and 400°C . This temperature range is consistent with values derived from the variation in the thickness of the mantle transition zone below the Society or Galapagos mantle hotspots [Niu et al., 2002; Hooft et al., 2003].

[12] Melting has been simply addressed by delimiting the regions where the solidus temperature is exceeded. We used the melting curves given by Katz et al. [2003] for anhydrous melting ($T_{\text{solidus},^\circ\text{C}} = 1085.7 + 132.9 P_{\text{Gpa}} - 5.1 P_{\text{Gpa}}^2$).

3. Results

[13] The behavior of plumes depends both on Ra and on the plume buoyancy flux, which in 2D may be estimated as $B = \int_{\Omega} \alpha \rho \Delta T v_z dx$, where Ω is the bottom of the model

(Figure 1). At low Ra , small plumes are entrained by the large-scale flow induced by plate motion and cannot reach the base of the lithosphere. When B is increased, plume material can ascend, but the conduit is deflected at depth by the large-scale flow and the plume reaches the basis of the lithosphere downstream from its original position (Figure 2a). At higher Ra , plumes are little perturbed by the large-scale flow and ascend easily throughout the upper mantle (Figure 2b). When the plume reaches the base of the lithosphere, most of the hot plume material flows downstream, entrained by the plate motion, and a plume-

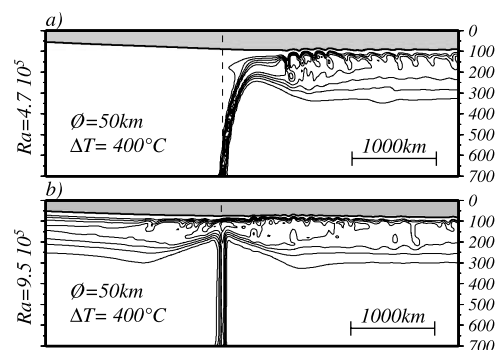


Figure 2. Isotherms characterizing the variation in plume behavior for a temperature perturbation ΔT of 400°C and a diameter \emptyset of 50 km at different Rayleigh numbers. Isotherms are drawn 50°C apart, starting at 1375°C . The lithosphere cooler than 1200°C is shaded.

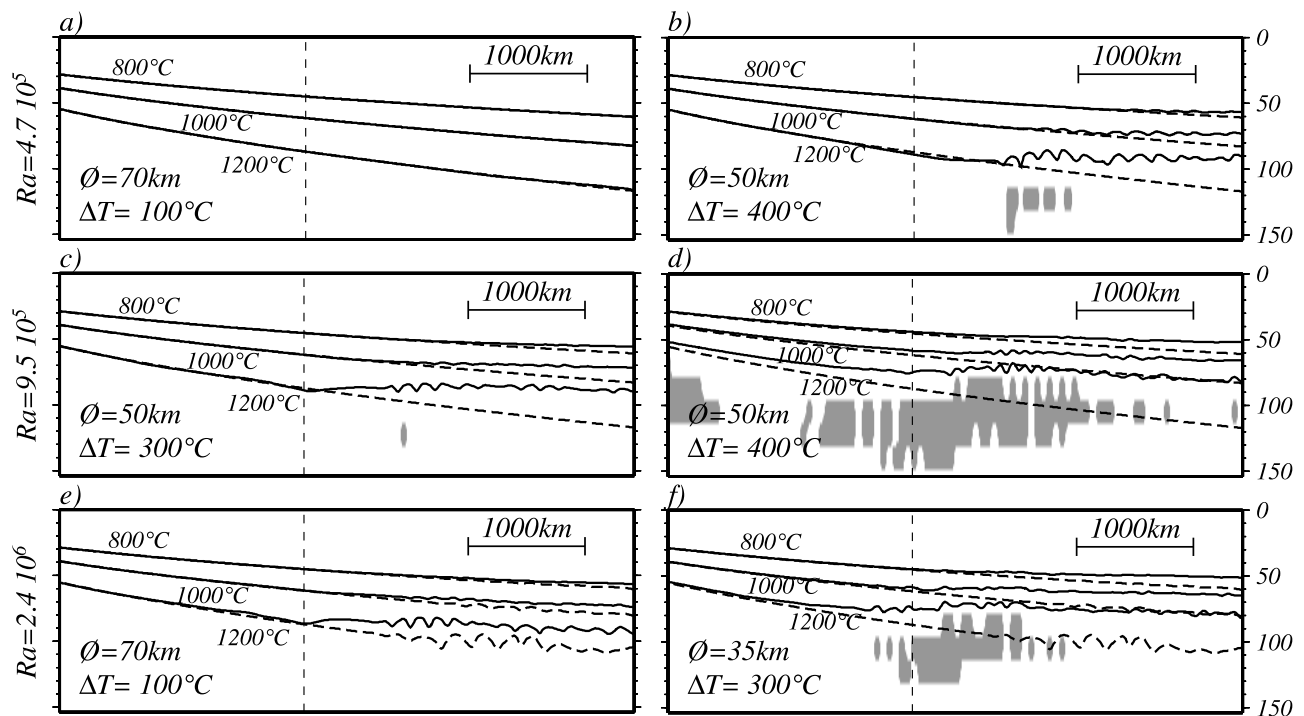


Figure 3. Erosion illustrated by the uplift of the 800°C, 1000°C and 1200°C isotherms (solid lines) relative to the initial equilibrium temperature distribution (dashed lines) for 6 combinations of Rayleigh number (increased from top to bottom) and plume buoyancy flux (increased from left to right). Values of Ra, plume diameter Φ , and temperature anomaly ΔT are indicated. Regions where anhydrous melting occurs are shaded.

lithosphere boundary layer develops where dripping instabilities can be observed (Figure 2). At high Ra and large B, a large part of the plume material moves upstream (Figure 2b), overrunning the large-scale convection flow. This behavior is probably shifted towards higher Ra and B in 3D.

[14] Plume-induced small-scale convection leads to thermal rejuvenation of the lithosphere. This is illustrated by the uplift of the 800, 1000, and 1200°C isotherms from their position at the initial equilibrium stage (Figure 3). Thinning of the lithosphere starts as soon as the plume material forms a low-viscosity layer in which a vigorous small-scale convection develops. At low Ra and weak plumes, it occurs downstream from the plume starting position (up to 1000 km, Figures 2a and 3b) because the plume conduit is deflected at depth. The flattening of the 1200°C isotherm downstream mimics a plate-like thermal structure. The thermal rejuvenation of the plate is controlled by the equilibrium thickness of the plate at the plume impact and by the thermal anomaly imposed by the plume. Erosion is effective even for small plumes. The 1200°C isotherm is displaced upwards by 10–40 km, but the 800°C isotherm is hardly perturbed in all cases. This results in a steep transient geotherm between 800 and 1200°C. The rejuvenated thermal structure is stable as long as the plume-induced thermal anomaly at the base of lithosphere is maintained. Return to the initial equilibrium shape will occur far downstream, when the plume-lithosphere boundary layer disappears. It is never observed within the modeled box.

[15] Melting occurs where the plume material is above the solidus. A plume with a small temperature anomaly ($<100^\circ\text{C}$) will not produce melting (Figure 3e), even if it

reaches and erodes the lithosphere. At low Ra, melting occurs downstream from the plume source (Figure 3b). For higher Ra, plumes ascend almost vertically and melting starts right above the plume conduit. In all cases, lithosphere erosion and melting start at the same point. At low Ra, the minimum temperature anomaly to produce melting is higher, because of deflection of the plume conduit (Figure 3b). A plume 50 km wide with a 400°C temperature anomaly, which only produces melting downstream at $Ra = 4.7 \cdot 10^5$ (Figure 3b), results in massive melting, starting straight above the plume conduit and extending far downstream and even upstream, at $Ra = 9.5 \cdot 10^5$ (Figure 3d). This amount of melting seems unrealistic for ongoing plumes. On the other hand, at $Ra = 2.4 \cdot 10^5$, a plume that overruns the large-scale flow does not melt (Figure 1).

4. Discussion

[16] The Rayleigh number and the corresponding mantle viscosity is an important parameter controlling the behavior of mantle plumes and, consequently, their erosional potential and the amount of melting. All plumes impinging the lithosphere induce small-scale convection and hence lithosphere erosion. Analysis of plume behavior and melting ability provides thus upper and lower bounds on upper mantle viscosity (Figure 1). For the high plate velocities investigated in this study (13.5 cm/y), plumes that reach the lithosphere and melt without overrunning the plate-induced flow place upper and lower bounds on Ra at $4 \cdot 10^5$ and $3 \cdot 10^6$, respectively. The corresponding viscosities at the base of the upper mantle are 10^{20} and 10^{21} Pa.s. Smaller plate velocities may result in similar behavior at lower Ra.

On the other hand, latent heat, which is not considered in the present models, may slightly displace these bounds towards higher values.

[17] Another key parameter is the plume buoyancy flux. Despite the trade-off between the temperature anomaly and the diameter of the plume, the “ideal” temperature anomaly appears to be in the range 250–400°C. It will be reduced (increased) for plumes beneath younger (older) hence thinner (thicker) lithosphere. Plumes diameters considered in this study are in the range of a few tens of kilometers. Wider plumes (200 km, 200°C) unrealistically overrun the plate-induced flow even at low Ra (Figure 1). This behavior will be reinforced at high Ra, suggesting that plume tails with diameters much larger than 100 km may be ruled out. This deduction contrasts with recent high-resolution tomographic models that image mantle plumes with diameters larger than 200 km [Montelli et al., 2004]. However, the present results have been obtained in a 2D geometry, which may lead to underestimation of plume diameters since it suppresses the divergent flow of plume material beneath the lithosphere.

[18] The present models show that plume-induced small-scale convection results in significant reheating of the lithosphere. Earth-like plumes (i.e., producing melt, but not disrupting the large-scale flow) induce up to 30 km of uplift of the 1200°C isotherm. Because of the fast motion of the plate, we observe flattening rather than local erosion of the lithosphere. This leads to plate-like subsidence downstream of the plume as observed for the South Pacific Superswell [Hillier and Watson, 2004], rather than the strong and localized thinning of the lithosphere inferred from receiver function data beneath the old Hawaiian islands [Li et al., 2004]. The modelled plume-induced small-scale convection is similar to the instabilities observed below oceanic plates at old ages in convection models at high Rayleigh number [Davaille and Jaupart, 1994; Dumoulin et al., 2001]. The final lithosphere thickness is thus controlled by the local Rayleigh number at the plume-lithosphere boundary layer, which depends on heat flux input by the plume and on the average asthenosphere viscosity.

[19] **Acknowledgment.** We thank Anne Davaille and an anonymous referee for careful review and suggestions that greatly improved our manuscript.

References

- Bock, G. (1991), Long-period S to P converted waves and the onset of partial melting beneath Oahu, *Geophys. Res. Lett.*, *26*, 1493–1496.
- Bonneville, A., R. P. V. Herzen, and F. Lucazeau (1997), Heat flow over Reunion hot spot track: Additional evidence for thermal rejuvenation of oceanic lithosphere, *J. Geophys. Res.*, *102*, 22,731–22,747.
- Christensen, U. (1983), Convection in a variable-viscosity fluid: Newtonian versus power-law rheology, *Earth Planet. Sci. Lett.*, *64*, 153–162.
- Christensen, U. (1984), Convection with pressure and temperature dependent non-Newtonian rheology, *Geophys. J. R. Astron. Soc.*, *77*, 242–284.
- Constable, S., and G. Heinson (2004), Hawaiian hot-spot swell structure from seafloor MT sounding, *Tectonophysics*, *389*, 111–124.
- Courtilot, V., A. Davaille, J. Besse, and J. Stock (2003), Three distinct types of hotspots in the Earth’s mantle, *Earth Planet. Sci. Lett.*, *205*, 295–308.
- Davaille, A. (1999), Simultaneous generation of hotspots and superswells by convection in a heterogeneous planetary mantle, *Nature*, *402*, 756–760.
- Davaille, A., and C. Jaupart (1994), Onset of thermal convection in fluids with temperature-dependent viscosity: Application to the oceanic mantle, *J. Geophys. Res.*, *99*, 19,853–19,866.
- Davies, G. F. (1994), Thermomechanical erosion of the lithosphere by mantle plumes, *J. Geophys. Res.*, *99*, 15,709–15,722.
- Dumoulin, C., M.-P. Doin, and L. Fleitout (2001), Numerical simulations of the cooling of an oceanic lithosphere above a convective mantle, *Phys. Earth Planet. Inter.*, *125*, 45–64.
- Duncan, R. A., and M. A. Richards (1991), Hotspots, mantle plumes, flood basalts, and true polar wander, *Rev. Geophys.*, *29*, 31–50.
- Hillier, J. K., and A. B. Watson (2004), “Plate-like” subsidence of the East Pacific Rise-South Pacific Superswell system, *J. Geophys. Res.*, *109*, B10102, doi:10.1029/2004JB003041.
- Hooft, E. E. E., D. R. Toomey, and S. C. Solomon (2003), Anomalous thin transition zone beneath the Galapagos hotspot, *Earth Planet. Sci. Lett.*, *216*, 55–64.
- Karato, S., and P. Wu (1993), Rheology of the upper mantle: A synthesis, *Science*, *260*, 771–778.
- Katz, R. F., M. Spiegelman, and C. H. Langmuir (2003), A new parameterization of hydrous mantle melting, *Geochem. Geophys. Geosyst.*, *4*(9), 1073, doi:10.1029/2002GC000433.
- Li, Y., R. Kind, X. Yuan, I. Wolbern, and W. Hanka (2004), Rejuvenation of the lithosphere by the Hawaiian plume, *Nature*, *427*, 827–829.
- Monnereau, M., M. Rabinowicz, and E. Arquis (1993), Mechanical erosion and re-heating of the lithosphere: A numerical model for hotspot swells, *J. Geophys. Res.*, *98*, 809–823.
- Montelli, R., G. Nolet, F. Dahlen, G. Masters, E. Engdahl, A. Robert, and S.-H. Hung (2004), Finite-frequency tomography reveals a variety of plumes in the mantle, *Science*, *303*, 339–343.
- Moore, W. B., G. Schubert, and P. J. Tackley (1998), Three-dimensional simulations of plume-lithosphere interaction at the Hawaiian swell, *Science*, *279*, 1008–1011.
- Niu, F., S. C. Solomon, P. G. Silver, D. Suetsugu, and H. Inoue (2002), Mantle transition-zone structure beneath the South Pacific Superswell and evidence for a mantle plume underlying the Society Hotspot, *Earth Planet. Sci. Lett.*, *198*, 371–380.
- Priestley, K., and F. Tilmann (1999), Shear-wave structure of the lithosphere above the Hawaiian hotspot from two-station Rayleigh wave phase velocity measurements, *Geophys. Res. Lett.*, *26*, 1493–1496.
- Ribe, N. M., and U. R. Christensen (1994), Three-dimensional modeling of plume-lithosphere interaction, *J. Geophys. Res.*, *99*, 669–682.
- Ribe, N. M., and U. R. Christensen (1999), The dynamical origin of Hawaiian volcanism, *Earth Planet. Sci. Lett.*, *171*, 517–531.
- Sleep, N. H. (1994), Lithospheric thinning by midplate mantle plumes and the thermal history of hot plume material ponded at sublithospheric depths, *J. Geophys. Res.*, *99*, 9327–9343.
- Steinberger, B. (2000), Plumes in a convecting mantle; models and observations for individual hotspots, *J. Geophys. Res.*, *105*, 11,127–11,152.
- Von Herzen, R. P., M. J. Cordery, R. S. Detrick, and C. Fang (1989), Heat flow and the thermal origin of the hot spot swells: The Hawaiian swell revisited, *J. Geophys. Res.*, *94*, 13,784–13,799.
- Woods, M. T., and E. A. Okal (1996), Rayleigh-wave dispersion along the Hawaiian Swell: A test of lithospheric thinning by thermal rejuvenation at a hotspot, *Geophys. J. Int.*, *125*, 325–339.
- Woods, M. T., J. J. Levêque, E. A. Okal, and M. Cara (1991), Two-station measurements of Rayleigh wave group velocity along the Hawaiian Swell, *Geophys. Res. Lett.*, *18*, 105–108.

M.-P. Doin, Laboratoire de Géologie, Ecole Normale Supérieure, 24 rue Lhomond, F-75231 Paris Cedex 5, France.

C. Thoraval and A. Tommasi, Laboratoire de Tectonophysique, Université Montpellier 2, Pl. E. Bataillon, F-34095 Montpellier Cedex 5, France. (catherine.thoraval@dstu.univ-montp2.fr)